Capacity of IEEE 802.11p based VANET: models, simulations and experimentations

Anh Tuan Giang, Anthony Busson, Alain Lambert, Dominique Gruyer

Capacity of IEEE 802.11p based VANET: models, simulations and experimentations

Anh Tuan GIANG
Laboratory of Signals and Systems
Université Paris Sud - Supélec - CNRS

Anthony BUSSON
Laboratoire de l'Informatique du Parallélisme (LIP)
University Lyon 1 - ENS-LYON - INRIA

Alain LAMBERT
IFSTTAR
IM, LIVIC
F-78000 Versailles, France

Dominique GRUYER
IFSTTAR
IM, LIVIC
F-78000 Versailles, France

***Abstract*—This paper aims to analyze two major quantities related to the performances of IEEE 802.11p based Vehicle Ad hoc NETwork (VANET): the mean number of simultaneous transmitters and the distribution of the distance between them. This first quantity is directly related to the network capacity as it limits the number of frames transmitted in the network at the same time. The second quantity is a crucial element to describe interference generated by the simultaneous transmitters and to deduce important wireless properties such as the Signal on Noise plus Interference ratio, Bit Error Rate or the Frame Error Rate. We propose two different models to approach these quantities: an extension of the Rényi's packing model and a Markovian point process. Theoretical propositions are compared to simulations performed with the Network Simulator NS-3. These simulations have been improved in two ways. The radio model has been set according to real experimentations. These experimentations involved two vehicles equipped with IEEE 802.11p wireless cards. Also, we implemented a realistic vehicles traffic simulator, emulating highway traffic, that we combined with NS-3.**

***Index Terms*—Vehicular ad hoc network, capacity, CSMA/CA.**

I. Introduction

Inter-Vehicular Communication (IVC) systems have the potential to greatly influence the road safety as well as to improve traffic flow by providing the drivers with critical route information. The IEEE 802.11p [1] standard (also referred to as Wireless Access in Vehicular Environments, WAVE) has been standardized to support these communications. This standard includes data exchanges in-between vehicles and between infrastructure and vehicles, using ad hoc mode. The network formed by the vehicles is called a Vehicular Ad hoc NETwork (VANET).

With the emergence of embedded sensors, a vehicle may collect information about its environment. The vehicle system can inform the driver about a local anomaly, a too short inter-distance with the leading vehicle. Also, it may help to adhere to road codes such as pavement marking, etc. Data from these sensors may be exchanged between vehicles in order to increase the perception of this environment. This extended vision may help the driver to take appropriate decisions [2]. For instance, inter-vehicle communications can be used to alert drivers about a dangerous situation, presence of an icy patch, an accident, etc. As a result, a timely warning may help the driver to avoid an emergency stop or sometimes, a collision [3]. Cooperative ITS applications will include safety, efficiency and value-added services, such as advertisements. However, it is primarily the traffic safety applications that will be allowed to use 802.11p.

But, all these applications have different bandwidth requirements. Dissemination of warning messages consumes a limited capacity as these applications generate a few sporadic messages. On the other hand, autonomous driving systems require a periodical exchanged of information from the embedded sensors. Estimation of VANET capacity is thus fundamental, as it may limit the deployment or the feasibility of such applications. Therefore, the capacity must be estimated a priori in order to design applications with the capacity constraint in mind.

This paper aims to study the network capacity defined as the number of bits that can be transmitted in average in one second

per unit of area. We do not consider multi-hop or unicast end-to-end throughputs. The remaining of this paper uses this definition of the capacity that can be different from the many definitions in the literature. The capacity of VANET using IEEE 802.11p standard is mainly limited by the spatial reuse. Indeed, in classical 802.11 based ad hoc networks, each node is equipped with only one network interface card, and all the nodes use the same channel. Therefore, this channel must be shared. Fortunately, when two vehicles/nodes are sufficiently far from each other, they can transmit at the same time without interfering. The possibility to reuse the medium at different geographical locations is the so-called spatial reuse. It can be illustrated through a simple example. Let us consider the vehicles distribution depicted in Figure 1. We assume that the current situation is a saturated communication case where all the vehicles wish to send a frame. The 802.11p MAC layer aims to select a subset of vehicles that will be allowed to transmit, such that the distances between concurrent transmitters is sufficiently great to avoid harmful interference between the transmissions. More precisely, a potential transmitter uses the CCA (Clear Chanel Assessment) mechanism to set if the medium is idle or not. This mechanism is detailed in the next section. The number of simultaneous transmitters (the number of red vehicles) sets the number of frames that can be transmitted at the same time. It is then used to evaluate the number of frames that can be sent per second, from which we deduce the capacity. Indeed, we modeled the number of transmitted bits, and implicitly assumed that it corresponds to the received ones. It corresponds to cases where receivers are sufficiently close to senders. Derivation of Frame Error Rates as function of transmitters-receivers distances and modulation schemes are out of scope of this paper. This capacity, sometimes called spatial capacity, depends on the area where nodes are scattered. We consider here a straight road or highway scenario. The obtained result is then normalized and expressed in Megabit per second and kilometer. This normalizing is done in order to present results as an estimate of the number of bits that can be exchanged on one km and in one second. We propose an extension of the Rényi's packing model [4] to estimate this normalized capacity. Our bound is based on favorable radio and traffic conditions, and offer an upper bound on this capacity. We shall show through a large set of simulations that this bound is achievable under certain assumptions, and keeps accurate when considering more complex scenarios on radio environment, data traffic, and traffic of vehicles. This bound may be used to limit the transmission rates of the VANET applications. For instance, for applications that performs regular broadcast at 1 hop, all the vehicles in the same kilometer will have to share this capacity. If we neglect the other applications, the application rate should thus be lower than this capacity divided by the density of nodes implementing this application (number of vehicles using this application in 1 km). When considering multi-hop communications, the capacity per kilometer must be divided by the number of sources and forwarders of this application.

The second quantity evaluated in this work is the distribution of the distance between the concurrent transmitters. This distance is modeled through a Markov chain taking its value in a continuous state space. The stationary distribution of this chain corresponds to the distribution of the distance between transmitters. It can help us to describe interference generated by the simultaneous transmitters, and to deduce important properties on the wireless link such as the Signal on Noise plus Interference ratio, or the Frame Error Rate.

Our approach has the advantage to model any technologies using CSMA/CA medium access control, even if our evaluations and simulations focus on the IEEE 802.11p standard. One important contribution of this paper is to propose accurate and reliable bound on the reachable capacity, that could be used as real dimensioning tools for VANET applications. The proposed models do not give a theoretical bound on the asymptotic capacity, but instead, offer a very realistic estimation of this capacity which can be reached in practice and in real conditions.

The paper is organized as follows. In Section II, the fundamental concepts and working mechanisms of IEEE 802.11p are described. Also, related works are summarized. Assumptions made in this paper which are common to our two models are described in Section III. The extension of the Rényi's packing model is presented in Section IV. The distribution of the distance between transmitters being intractable with this model, we propose a Markovian model in Section V. In Section VI, we describe the experimentations we made with a set of vehicles equipped with IEEE 802.11p interfaces. These experimentations are used to obtain realistic radio models for VANET. Also, we used a traffic generator emulating realistic vehicle trajectories on a highway. Both radio model and traffic simulator have been integrated in the network simulator NS-3 [5] to perform simulations as realistic as possible. Theoretical and simulation results are compared and discussed in Section VII. Finally, we conclude in Section VIII.

II. BACKGROUND

A. IEEE 802.11p CSMA/CA

The IEEE 802.11p standard was built based on DSRC (Dedicated short-range communications) standard, a successor of ASTM E2213-03 (Standard Specification for Telecommunications and Information Exchange Between Roadside and Vehicle Systems). The physical layer is composed of Service Channels (SCH), and a Control Channel (CCH), working in 5.9 GHz band. SCH channels are reserved for common applications, whereas CCH channel is dedicated for privilege applications, especially high priority applications like safety and warning. The MAC layer of 802.11p manages different priorities according to the IEEE 802.11e standard. It has 4 queues for different type of messages. These queues contend internally before a transmission. Each queue has a different set of parameters in order to respect the priority. After finishing the internal contending phase, the node applies the CSMA/CA protocol to access the medium for the selected frame. It began by sensing the medium to check if it is busy or not. The CCA *Clear Channel Assessment* mechanism will be summoned for this purpose. Depending on the channel state, idle or busy, the transmission is started or postponed. CCA mode and

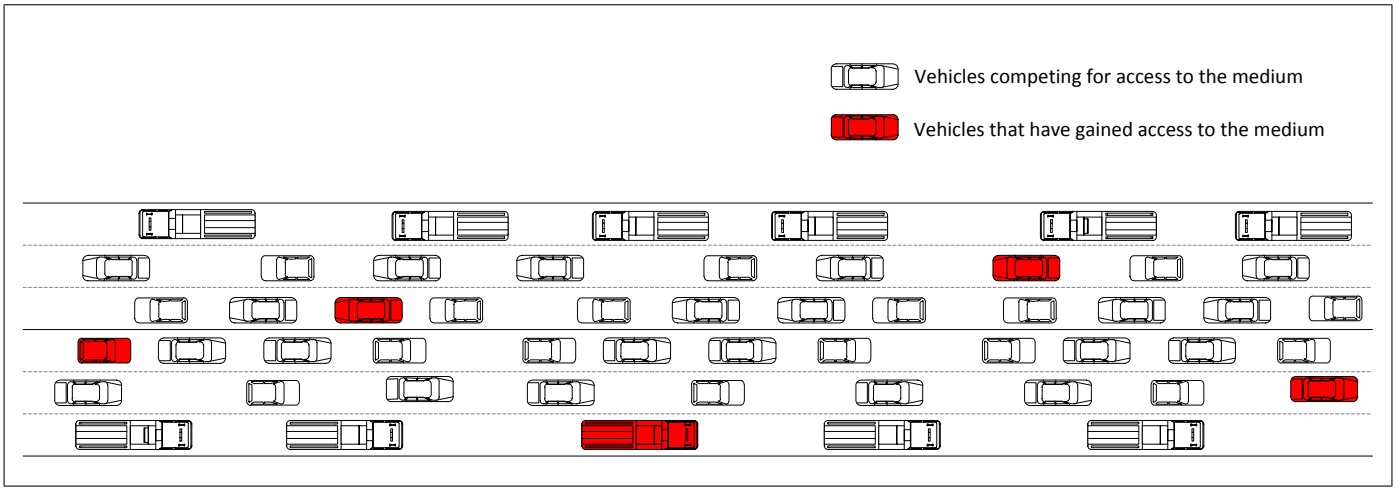

Fig. 1. Example of concurrent transmissions: the 802.11p MAC layer (CSMA/CA) set the rules to access the medium. Only red vehicles are allowed to transmit frames at the same time

parameters depend on the MAC protocol and the terminal settings. CCA is performed according to one of these three methods:

1) CCA Mode 1: *Energy above threshold*. CCA shall report a busy medium upon detecting any energy above the Energy Detection (ED) threshold. In this case, the channel occupancy is related to the total interference level.
2) CCA Mode 2: *Carrier sense only*. CCA shall report a busy medium only upon the detection of a signal compliant with its own standard, i.e. same physical layer (PHY) characteristics, such as modulation or spreading. Note that depending on threshold values, this signal may be above or below the ED threshold.
3) CCA Mode 3: *Carrier sense with energy above threshold*. CCA shall report a busy medium using a logical combination (e.g. AND or OR) of Detection of a compliant signal AND/OR Energy above the ED threshold.

The CCA mechanism aims to ensure that there is a minimal distance between simultaneous transmitters. It is performed at the transmitter, and cannot guarantee in practice a low interference level at the receiver: a receiver may suffer from harmful interference even if the medium was detected idle (by the transmitter). The CCA is strongly linked to the radio environment and obstacles that may be located between a transmitter and a node performing the CCA mechanism. In this paper, the path-loss function used in the numerical evaluation assumes line of sight transmissions, i.e. does not model obstacles. Nevertheless, our model could be adapted to take into account these obstacles through more complex path-loss functions.

The CCA mechanism limits the number of simultaneous transmitters in a given area, and thus the number of frames that can be sent per second. Therefore, there is a direct relationship between the spatial reuse imposed by the CCA mechanism and the capacity.

B. Related works

A theoretical bound on the capacity of ad hoc networks was initially investigated in [6] where the authors prove that, in a network of n nodes, a capacity of $\Omega\left(\frac{1}{\sqrt{n \cdot \log n}}\right)$ is feasible. This pioneering work has been extended in a great number of studies [7], [8], [9]. In these articles, the capacity is reached by means of particular transmission scheduling and routing schemes, with more or less elaborated radio models. The obtained results is an estimation of the asymptotic capacity, which is shown $O\left(\frac{1}{\sqrt{n}}\right)$, or $O\left(\frac{1}{n}\right)$ depending on the radio models and routing schemes. The route throughput taken into account spatial reuse has been studied in [10]. A capacity estimation, specific to CSMA/CA ad hoc networks, has also been investigated in [11].

All these studies focus on networks where nodes are distributed on the plane or in a 2-dimensional observation window. VANETs have very different topologies as the vehicles/nodes are distributed along roads and highways. Radio range of the nodes (about 700 meters with 802.11p in rural environment) being much greater than the road width, we can consider that the topology is distributed on a line rather than in a 2 dimensional space. Lines, grids or topologies composed of a set of lines (to model streets in a city) are thus more appropriate to model VANET topologies.

The capacity of 802.11p wireless link in a VANET has been evaluated in [12], [13], [14]. They estimate the maximum capacity between two vehicles communicating with each other's, but it does not give the global capacity of the network considering sharing and spatial reuse of the medium. In [15], [16], [17], the authors propose a bound on VANET capacity. They show that when nodes are at constant intervals or randomly distributed along a line, the capacity is $O\left(\frac{1}{n}\right)$ and $O\left(\frac{1}{n \cdot ln(n)}\right)$ in downtown (city) grids. But it is an asymptotic bound. In [18], the broadcast capacity of a VANET is estimated. The idea is similar to our paper: an estimation of the number of simultaneous transmitters is proposed. The evaluation is only based on numerical evaluation, using integer programming. In [19], authors proposed a model to compute

the mean number of simultaneous transmitters in a linear VANET. An upper and lower bound for the capacity had been derived. However, interference is not taken into account, and the distance distribution between concurrent transmitters is not developed.

III. Assumptions

Our proposed models mimic the CCA mode 1, where the sum of signals from all transmitters is taken into account to detect the medium idle or busy. With this mode, a node will be allowed to transmit its frame if the measured interference is lower than a pre-defined threshold θ. We consider a path-loss function $l(.)$, which gives the reception power of a signal as function of the distance from the transmitter. We assume that $l(.)$, defined in $\mathbb{R}^+$, is positive, continuous, decreasing, $l(0) > \theta$ (θ is the CCA threshold) and $\lim_{u\to+\infty} l(u) = 0$. It holds in particular for classical path-loss functions with the form: $l(u) = P_t\ min(1, c/u^\alpha)$ where P_t is the transmitting power (with $P_t > \theta$), and c and α are two positive constants. We shall use this family of path-loss functions in our evaluations, but any deterministic path-loss functions verifying these conditions could be considered instead. Our different results are linked to these functions through simple equations presented in Sections IV-C and V.

Also, we assume that interference $I(x)$ at x ($x \in \mathbb{R}^+$) is generated by the two closest transmitters:

$$I(x) = l(x - Le) + l(Ri - x) \quad (1)$$

where Le, Ri are the two closest transmitting nodes around x, the closest one on the left (located at Le) and on the right (located at Ri). With the IEEE 802.11p expected performances, this model is very similar to a model where interference from all the transmitters is taken into account. Indeed, as there is a significant distance between two successive transmitting nodes (due to the CCA mechanism), interference generated by distant interferers is negligible with regard to the closest ones (with the maximal transmitting power of 802.11p and in a rural environment, the second interferer in a given direction will be at least 1 km away from the first one). Therefore, according to CCA mode 1, a node at x detects the medium idle and can transmit a frame, if and only if:

$$I(x) = l(x - Le) + l(Ri - x) < \theta \quad (2)$$

IV. An extension of the Rényi's Packing Model

Before presenting our extension of the Rényi's model, we present the classical one.

A. Classical Rényi's packing model

Let assume that a transmission is detected if the distance from the transmitter is less than a pre-defined distance R. It means that if there is a transmitter at location x, other nodes within the segment $[x - R, x + R]$ cannot access the medium. With this simple assumption, the problem about determining the maximum number of simultaneous transmitters comes down to the following question: how many segments with size $2R$ can we put in a certain interval $[a, b]$ under the constraint that the centers of these segments cannot be covered by another segment? We consider a model in which these segments will be located randomly in $[a, b]$. The first segment is placed uniformly in $[a, b]$. Then, we place the second segment uniformly into all points t of [a,b] such that a segment at t does not cover the center of the previous segments, and so on. The process terminates when there are no gaps in $[a, b]$ large enough to host another segment. This model is referred to as the Rényi's packing problem [4]. A rigorous analysis [4] shows that the mean number of segments multiplied by the segment length ($2R$) and divided by the interval length ($b-a$) tends to a constant $\gamma \approx 1.4952$ when $(b - a) \to +\infty$. The number of simultaneous transmitters can then be estimated as $(b - a)\frac{\gamma}{2R}$ for $(b - a)$ large enough.

The Rényi's model can be applied in the case where only the closest interferer (but not the sum of signals from L_e or R_i) is taken into account. The detection distance R may be deduced from the path-loss function, i.e. the distance at which the signal strength generated by a transmitter is equal to the

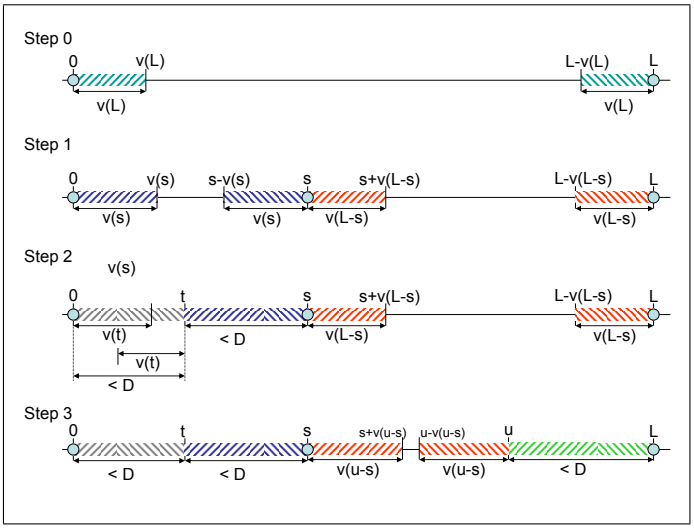

Fig. 2. A sample of our model.

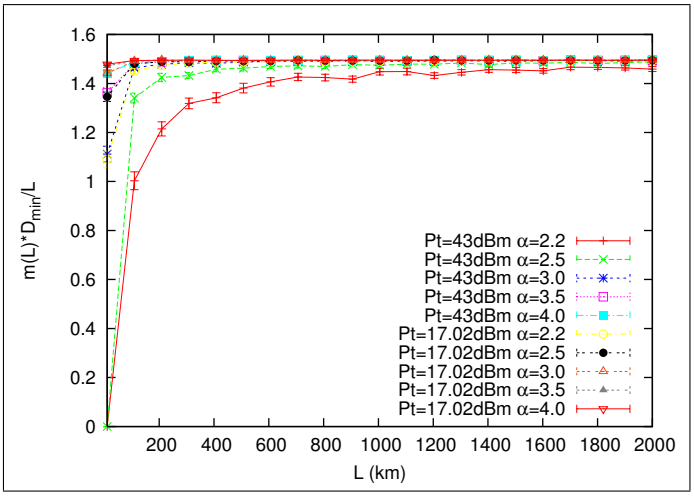

Fig. 3. Convergence of $\frac{m(L)D}{L}$ as L increases for $l(u) = P_t.min(c, \frac{c}{u^\alpha})$ and different value of α and P_t. D is the solution of $2l(\frac{D}{2}) = \theta$ with $\theta = -99dBm$.

ED threshold ($l(R) = \theta$).

B. Extension of the Rényi's packing model

Our extension aims to take into account interference in the selection of the transmitters rather than a deterministic distance. We consider a highway or a road with length L. The interval is thus $[0, L]$. The model gives the maximum number of transmitters in $[0, L]$ such that the CCA rule given by Equation (2) is respected.

Around each transmitter there is an inhibition interval where the interference level (sum of the signal given by Equation (2)) is above θ. These intervals correspond to the hatched rectangles in Figure 2. They are asymmetric: inhibition intervals are different on the left and right hand sides of a transmitter. We use a function $v(s)$ to describe their lengths. If s ($s > 0$) represents the distance between two consecutive transmitters, the interference level for a point at distance u from one of these transmitters will be $l(u)+l(s-u)$. The minimal distance $v(s)$ from these transmitters that verifies Equation (2) is thus defined by:

$$l(v(s)) + l(s - v(s)) = \theta \tag{3}$$

This equation makes sense only if s is sufficiently great ($s > 2 \cdot v(s)$). This minimal length is denoted D with D solution of $2 \cdot l(\frac{D}{2}) = \theta$. The function $v(.)$ is thus defined in $[D, +\infty]$.

We can now describe the process to set the transmitter locations. We assumed that there are two initial transmitters at locations 0 and L. If $L > D$, a new transmitter is uniformly distributed in $[v(L), L-v(L)]$. Let s be its location. If $s > D$, a new point is uniformly distributed in $[v(s), s - v(s)]$, and if $L - s > D$ a new point is uniformly distributed in $[s+v(L-s), L-v(L-s)]$. Each time a new point is added, it creates a new interval on its left and its right. If the length of an interval is less than D we cannot add a new point, otherwise we add a new point uniformly distributed in this interval. The process stops when all intervals are smaller than D. An example of this process is represented in Figure 2:

- Step 0 (initialization): two nodes are located at 0 and L.
- Step 1: a new point is uniformly distributed in $[v(L), L-v(L)]$, at s in our example. There are two new intervals where transmitters can be added : $[0, s]$ and $[s, L]$. In our example, they are both greater than D. Taking into account the inhibition intervals, new transmitters can be distributed in $[v(s), s-v(s)]$ and $[s+v(L-s), L-v(L-s)]$.
- Step 2: a new point is uniformly distributed in $[v(s), s-v(s)]$. It is located at t. Interval on the left and right of t are smaller than D. Therefore, points cannot be added in these two intervals.
- Step 3: a new point u is uniformly distributed in $[s + v(L-s), L-v(L-s)]$.
- Step 4: The interval on the right hand side of u is smaller than D. But a new point can be added on the left, in the interval $[s + v(u-s), u-v(u-s)]$. It is not shown in the figure. This last point terminates the process.

We denote $m(L)$ the mean number of points in the interval $[0, L]$ at the end of the process. $m(L)$ does not count the two initial points at 0 and L. Unfortunately, its computation is, to our knowledge, intractable. Nevertheless, we can prove its convergence.

Proposition 1. *Let $m(L)$ be the mean number of points in the interval $[0, L]$ for the process defined above, then:*

$$\lim_{L \to +\infty} \frac{m(L)}{L} = \lambda \tag{4}$$

where λ is a positive constant.

The proof is given in Appendix. This proposition proves that the intensity of this point process converges to a constant as the size of the interval increases. This constant can be used to evaluate the mean number of simultaneous transmitters and the capacity of the VANET. Indeed, $m(L)$ can be evaluated as λL. Consequently, the mean number of frames sent per second in the network can be estimated as:

$$\frac{\lambda L}{T} \tag{5}$$

where T is the mean time to transmit a frame. T totals the time to access to the medium, and the time to transmit the frame.

C. Estimation of λ and the capacity

According to Equation (5), estimation of the capacity boils down to the computation of the limit λ. We propose an estimation of λ that can be deduced directly from the path-loss function. In Figure 3, we plotted the quantity $\frac{m(L)D}{L}$ when L increases. It has been obtained by simulations of the model. Each point is the average of 100 samples and is shown with a confidence interval at 95%. The considered path loss function is $l(u) = P_t \cdot min(c, \frac{c}{u^\alpha})$, where P_t is the transmission power, c is the loss reference parameters (equals to -46.6dBm) and α is the path-loss exponent. In this figure, we took into account two transmitting powers $P_t = 17.02$dBm and $P_t = 43$dBm corresponding to transmission powers used in $802.11a$ and $802.11p$ technologies, and different path-loss exponent α modeling different radio environments. We observe that all curves converge to the same constant, approximately equals to 1.49. This result is not surprising as it holds for other packing problems in one or two-dimensional spaces (see [20] or [11] for instance). Also, we performed the same simulations for other path-loss functions (with exponential decay for example), and observe a convergence to the same constant. These results are not shown here because of the redundancy. This convergence to a universal constant allows us to estimate the limit λ of Proposition 1 as follows:

$$\lim_{L \to +\infty} \frac{m(L)}{L} = \lambda \approx \frac{\gamma}{D} \tag{6}$$

with $\gamma = 1.49$ and D solution of $2l(\frac{D}{2}) = \theta$. The final capacity, expressed in Mbps/km, is then evaluated as:

$$Capacity(L) = \frac{\gamma L \, Packet\_Size}{DT} \tag{7}$$

For a path-loss function with the form $l(u) = P_t \; min(1, c/u^\alpha)$ with $P_t c > \theta$, $2l(\frac{D}{2}) = \theta$ leads to

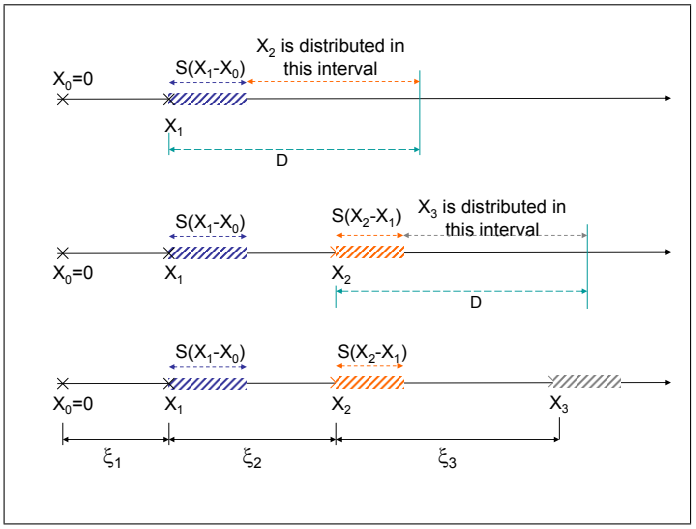

Fig. 4. Notations used in the model. The figure shows how the points X_2 and X_3 are distributed.

$D = 2\left(\frac{2P_t c}{\theta}\right)^{\frac{1}{\alpha}}$. The capacity per kilometer ($L = 1$km) is then $\frac{\gamma}{2T}\left(\frac{\theta}{2P_t c}\right)^{\frac{1}{\alpha}}$ with $\gamma = 1.49$. An example of computation of T is given in Section VII.

Even if our model considers variable interval lengths, it seems that the constant γ fit to the Rényi packing constant introduced in Section IV-A. An interesting extension of this work would consist in proving that these packing constants are effectively the same.

Equation (7) estimates the number of bits transmitted at the MAC layer under the energy detection mechanism. Therefore, it is a upper bound of the achievable capacity. The measured capacity is generally lower due to contention, collisions, and fading. Also, our estimation holds for a great density of vehicles, as it assumed that the medium is busy everywhere (busy according to the CCA mode 1). In practice, sections of road without potential transmitters will reduce this capacity. Section VII compares this bound with simulations that take into account realistic models in terms of data traffic, radio environments, and traffic of vehicles.

V. A Markovian Point Process

Extension of the Rényi packing model gives us a very simple and precise formula to estimate the capacity of VANET. However, we cannot acquire any information on the distribution of distances between the concurrent transmitters. This quantity is one of the major quantities involved in the computations of link properties such as $SINR$, BER and FER. Therefore, we propose in this section, a new model based on a Markovian Point Process. The model consists in a general Markovian point process composed of an ordered sequence of points $(X_n)_{n\geq 0}$ with $X_n \in I\!R^+$ which verifies two packing constraints. The first constraint is the packing criterion that sets the repulsion rule between the points. The second criterion ensures that the space is completely filled, and that it is impossible to add new points/transmitters.

- Criterion 1: the interference level at each point X_n of the point process (given by Equation (1)) is less than the Energy Detection threshold θ. Here, the interference computation does not take into account the signal from X_n. Indeed, X_n has detected the medium idle before transmitting.
- Criterion 2: the interference level at any point of $I\!R^+ \backslash \{X_n\}_{n\geq 0}$ (everywhere except at the transmitter locations) is greater than θ.

In the following, we define the interval where the random variables of the Markov chain take their values. It is set according to these two criteria. Then, we present the algorithm used to build the point process, and we give the particular transition density function used in this paper and the main results (in Proposition 2).

A. State space of the Markov chain

The chain is denoted $(X_n)_{n\in I\!N}$ with $X_{n-1} < X_n$. It represents the simultaneous transmitters of a CSMA/CA network and consists in a sequence of random points distributed on the line. According to Criterion 1, interference at each point X_n must be less than the CCA threshold θ:

$$I(X_n) < \theta \ \ \forall n \geq 0$$

But, the building of this point process does not mimic the Rényi model where a point is added according to the distance from the points on the left and on the right. Indeed, the points are added in an increasing way (X_n before X_{n+1} with $X_n < X_{n+1}$). X_n is thus set without the knowledge of the next transmitter location X_{n+1}, and the interference level at X_n is computed once the point X_{n+1} is set. Therefore, when we add a new point X_{n+1}, we need to take into account the interference level at the previous one (X_n), i.e. X_{n+1} must not increase interference at X_n above θ:

$$l(|X_n - X_{n-1}|) + l(|X_{n+1} - X_n|) < \theta \tag{8}$$

The minimal distance between X_n and X_{n+1} is denoted $S(|X_n - X_{n-1}|)$. The function $S(.)$ defines the minimal distance to the next transmitter. It is formally defined as the solution of

$$l(u) + l(S(u)) = \theta \tag{9}$$

where u corresponds to the distance between the two previous points/transmitters. A point X_n is thus distributed in $[X_{n-1} + S(X_{n-2} - X_{n-1}), +\infty]$.

The second criterion allows us to bound this interval. According to Criterion 2, we shall distribute the points in such a way that it is not possible to add more points which could detect the medium idle. Consequently, the distance between transmitters must be bound by a maximal distance in order to prevent the presence of intermediate transmitters. Let D be this distance, it is solution of

$$2 \cdot l\left(\frac{D}{2}\right) = \theta \tag{10}$$

D is the same quantity as the one defined in the packing model. Thus, each point X_n ($n > 1$) belongs to the interval $[X_{n-1} + S(X_{n-1} - X_{n-2}), X_{n-1} + D]$. Distances between the successive transmitters are denoted $\xi_i = X_i - X_{i-1}$. ξ_n ($n > 1$) is thus distributed in $[S(\xi_{n-1}), D]$.

B. Building the point process

The point process is built as follows. The first two transmitters are located at $X_0 = 0$ and at X_1 with $X_1 \leq D$ almost surely. Assumptions about the distribution of X_1 are given in Proposition 2.

The other points are built recursively. The location of a transmitter X_n ($n > 1$) is distributed in $[X_{n-1} + S(X_{n-1} - X_{n-2}), X_{n-1}+D]$. For convenience, we consider the sequence $\xi_n = X_n - X_{n-1}$ rather than X_n. The sequence $(\xi_n)_{n\geq 0}$ is thus a homogeneous Markov chain which takes its values in the continuous state space $[S(D), D]$. It is possible to consider any distribution on this interval, each one leading to different density of transmitters. The model can thus be adapted with regard to the system. For example, if we choose ξ_n as deterministic with $\xi_n = S(D)$ (respectively $\xi_n = D$), we obtain the maximum (respectively minimum) density of points verifying the two packing criteria. In Figure 4, we present an example of this point process and the different notations.

As we do not know a priori the transition density of the distance between the transmitters for our particular problem, we have considered different distributions. We have chosen to show only the most accurate distribution. It has been determined by comparison with NS-3 simulations (shown in the next sections). This distribution is the linear distribution in $[S(\xi_{n-1}), D]$. By linear distribution we mean an affine function, positive in $[S(\xi_{n-1}), D]$, null at D, and such that its integral on $[S(\xi_{n-1}), D]$ is 1. The pdf $f_{\xi_n|\xi_{n-1}}(.)$ of ξ_n given ξ_{n-1} is then:

$$f_{\xi_n|\xi_{n-1}=s}(u) = \Big(\frac{-2}{(D-S(s))^2}u + \frac{2D}{(D-S(s))^2}\Big)1_{u\in[S(s),D]} \qquad (11)$$

where $1_{u\in[S(s),D]}$ is the indicator function, equals to 1 if $u \in [S(s), D]$ and 0 otherwise. The stationary distribution of this Markov chain is given in the following proposition:

Proposition 2. *The process $(\xi_n)_{n\geq 0}$ defined in this Section is a Markov chain. The stationary distribution of ξ_n for the particular density transition function given by Equation (11) is $\pi(s)$ with:*

$$\pi(s) = a \cdot (D-s)(D-S(s))^2 1_{s\in[S(D),D]} \qquad (12)$$

where a is a normalizing factor. The chain $(\xi_n)_{n>0}$ converges in total variation to the distribution $\pi(s)$ for all initial distribution of ξ_1 in $[S(D), D]$. If ξ_1 follows the stationary distribution $\pi(.)$ then ξ_n follows the distribution $\pi(.)$ for all n with $n > 0$.

The proof of this proposition is given in the appendix. This function $\pi(.)$ represents the distribution of the distances between concurrent transmitters. According to numerical evaluations, the intensity of transmitters given by the packing model described in the previous section is lightly greater than the intensity of this process (given by the inverse of the mean distance). The previous bound is more precise as the model mimics quite accurately the algorithm used to access the medium. But, for this Markov model, we need to set a transition function that is a priori unknown, and that introduces a light bias. However, this second model allows us to estimate the distance distribution between transmitters that is not tractable with the packing model.

Fig. 5. Satory's speed track.

Fig. 6. Renault Clio III equipped vehicles (TIC and TAC) on the track.

VI. EXPERIMENTATIONS

Our theoretical models aim to provide precise tools to estimate VANET capacity. Unfortunately, estimation of the

Fig. 7. TIC's embedded equipments.

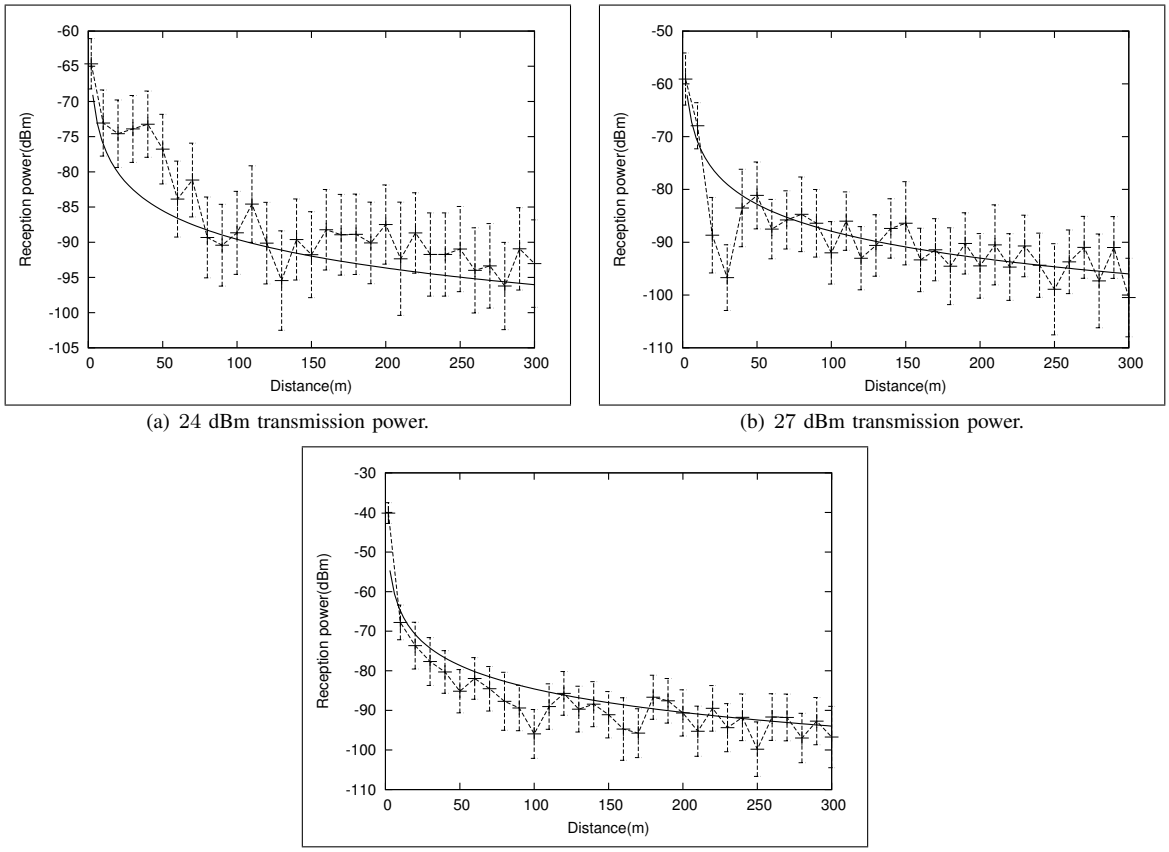

(a) 24 dBm transmission power.

(b) 27 dBm transmission power.

(c) 30 dBm transmission power.

Fig. 9. Path-loss function.

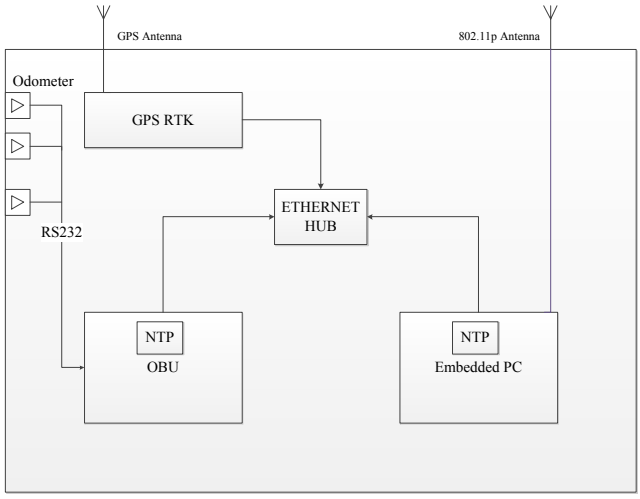

Fig. 8. Inside vehicle devices modules.

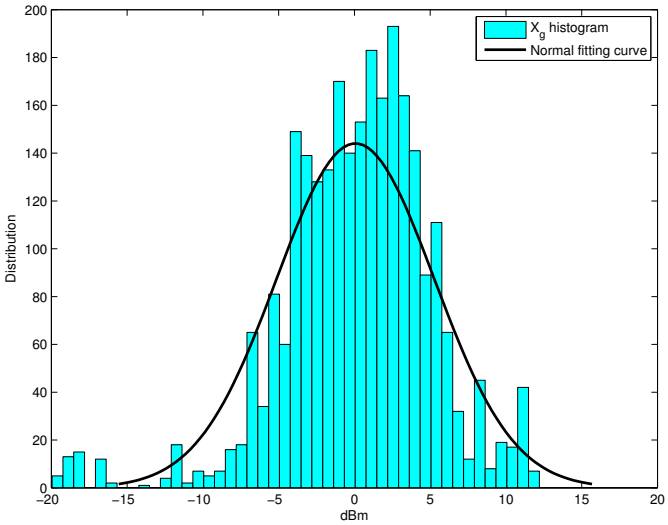

Fig. 10. X_g fading histogram and fitting curve ($T_x = 30$ dBm).

Transmission power	Exponent	Loss reference
24 dBm	1.3519	-86.5457 dBm
27 dBm	1.6964	-80.9766 dBm
30 dBm	1.9596	-75.1781 dBm

TABLE I
ESTIMATED PARAMETERS.

Transmission Power	24 dBm	27 dBm	30 dBm
Mean	0.06	-0.13	0.26
Standard deviation	5.2	5.07	5.24

TABLE II
NORMAL FITTING CURVE VALUES.

real spatial capacity was impossible as it requires a lot of vehicles scattered on roads of several kilometers. Consequently, we use a realistic simulator (presented in the next section) fed with a radio model whose parameters are obtained from experimentations. Such experimentations have already been perfomed [21], [22], but we wanted to assess path-loss functions and communication characteristics for recent 802.11p products.

We made experimentations on a track where vehicles were in the line-of-sight of each other's. Therefore, we considered a radio model that mainly depends on a path-loss function. Experimentations were thus used to estimate a realistic path-loss function, including distribution and parameters of a random variable modeling fading.

Experimentations took place on the Satory's speed track dedicated for testing vehicles, isolated from regular traffic. The speed track includes a 1 kilometer way of direct line of sight (see Figure 5). Two Renault Clio III vehicles (TIC : "*Transport Intelligent Coopératif*" and TAC : "*Télécommunication pour l'Assistance à la Conduite*") had been used for the experimentations. Figure 8 presents the block diagram of the different modules installed in the two vehicles. There is an On Board Unit (OBU) that collects and processes all data from the sensors (gyro, accelerometer, odometer, etc). IEEE 802.11p wireless interfaces which use Atheros 5413 Wi-Fi chipset were installed in an embedded PC (see the white box with the antenna on Figure 7). This computer operates under the Linux Ubuntu operating system. We installed the open-source ath5k Wi-Fi driver [23], which was patched in 2010 for the Grand Cooperative Driving Challenge [24] in order to enable 802.11p channels. Some modifications on the transmission power and frequencies have been made to adapt the compatibility of European Telecommunications Standards Institute [25]. Indeed, these devices were manufactured for United States market under Federal Communications Commission [26] Standards. An antenna with the gain of 3 dBi was connected to the embedded PC. An Ethernet interface was used to connect this embedded PC to the OBU (see Figure 8). The first vehicle (TIC) broadcasted the packets to the TAC vehicle that was set up as a server. For each received packet, it measured the reception power.

The main difficulty in this experimentation was to associate the packets with the distances. In other words, the TAC vehicle must know, for each packet, the distance from itself to the TIC vehicle. The location of a vehicle was computed thanks to a data fusion process (an Extended Kalman Filter using the embedded sensors including the RTK GPS [27]) allowing the OBU to achieve a centimeter precision on the distance. The location of the client (TIC) was time stamped and inserted in the packets sent to the server (TAC). The clocks of the OBU and the embedded PC were synchronized via the Network Transfer Protocol, according to the time of the GPS receiving module (see Figure 8). Consequently, we could associate the positioning informations and the reception powers.

We varied the distance between vehicles from 0 to 300 meters with a step of 10 meters. We collected at least 30 samples for each distance. We performed our experimentations with 3 different transmission powers: 24, 27 and 30 dBm. Since we considered a line-of-sight propagation model, we extrapolate the measured path-loss function with the classical Log Distance Path-loss model. The formula of this model is as follows:

$$R_x = T_x + LossRef - 10\alpha log(d) + X_g \qquad (13)$$

where R_x is the reception power, T_x is the transmission power, $LossRef$ is the loss reference, α is the path-loss exponent, d is the distance between transmitter and receiver and X_g is a random variable which models fading.

The elements that we need to estimate are $LossRef$, the path loss exponent α and the distribution of X_g. First, we assumed that $X_g = 0$. It allowed us to estimate $LossRef$ and α with a Minimum Mean Square Error (MMSE) method. Results are presented in Figure 9. It shows the mean reception power from the experimentations (with a 95% confidence interval) and the estimated path-loss function. The extrapolated parameters are summarized in Table I. Then, fading X_g was interpreted as the difference between the estimated path-loss function and the measured reception power (for each sample). The empirical distribution of X_g is shown in Figure 10 for a transmission power of 30 dBm. The best fit corresponds to a Normal distribution where parameters are given in Table II.

VII. SIMULATIONS

In order to estimate the accuracy of our approach, we present a comparison between simulations performed with the Network Simulator NS-3 [5] and our theoretical models. This section is composed of three parts. It begins by describing the different components of our simulators and their parameters. Then, the simulated capacity is compared to the one obtained with our extension of the Rényi model presented in Section IV. The last part is dedicated to the comparison of the transmitter inter-distances between simulations and the Markov model developed in Section V.

A. Simulators and parameters

Nodes are equipped with IEEE 802.11p interfaces. Each node is a CBR (Constant Bit Rate) source. This CBR rate is close to the 802.11p rate (6Mbps) in order to saturate the network. The capacity is computed as the number of bits that is properly received by the closest neighbor from the sender, and upstream with regard to the traffic. There are two simulation scenarios:

- *No fading case:* This scenario corresponds to NS-3 default models and parameters of the IEEE 802.11p technology. We neglected fading effect in this case. This radio model is equivalent to the one considered in our models. The other parameters are given in Table III.
- *Scenario from experimentations:* This scenario uses the radio model set from the experimentations (presented in Section VI). Fading is thus taken into account. It leads to a smaller radio range compared to the previous scenario. All parameters are given in Table IV.

We simulated a 20 km highway. To avoid edge effects, we did not take into account data from the first and the last 2.5 km

Theoretical and NS-3 Parameters	Numerical Values	Theoretical and NS-3 Parameters	Numerical Values
IEEE 802.11std	802.11p - CCH channel	Path-loss function	$l(d) = P_t \cdot min\left(1, \frac{10^{-4.5667}}{d^{3.0}}\right)$
CCA mode	CCA mode 1	ED Threshold (θ)	-99 dBm
Emission power P_t	43 dBm	Number of samples per point	100
Length of the packet	400 bytes	Duration of the simulation	4 sec
Road length	20 km		

TABLE III
SIMULATION PARAMETERS: NO FADING CASE.

Theoretical and NS-3 Parameters	Numerical Values	Theoretical and NS-3 Parameters	Numerical Values
IEEE 802.11std	802.11p - CCH channel	Path-loss function	$l(d) = P_t \cdot min\left(1, \frac{10^{-7.517}}{d^{1.9596}}\right)$
CCA mode	CCA mode 1	ED Threshold (θ)	-99 dBm
Emission power P_t	30 dBm	Number of samples per point	100
Length of the packet	400 bytes	Duration of the simulation	4 sec
Road length	20 km		

TABLE IV
SIMULATION PARAMETERS: SCENARIO FROM EXPERIMENTATIONS (WITH FADING).

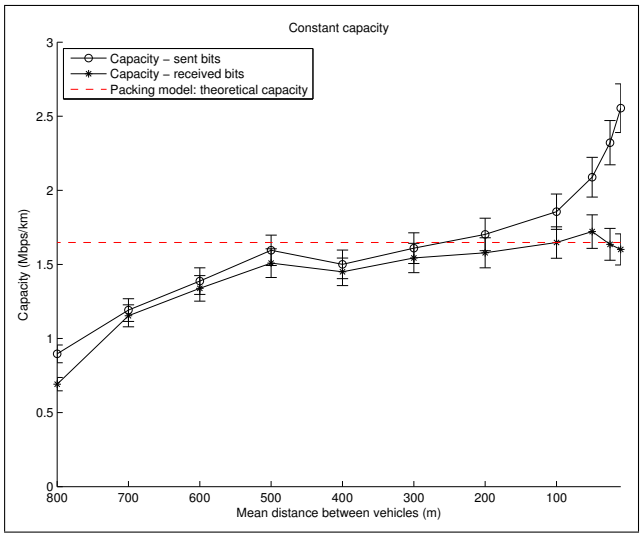

(a) Constant inter-distance.

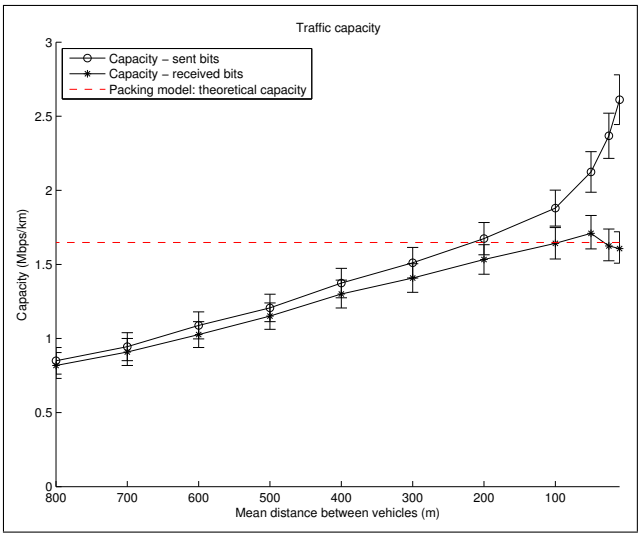

(b) Traffic simulator.

Fig. 11. No fading case: capacity.

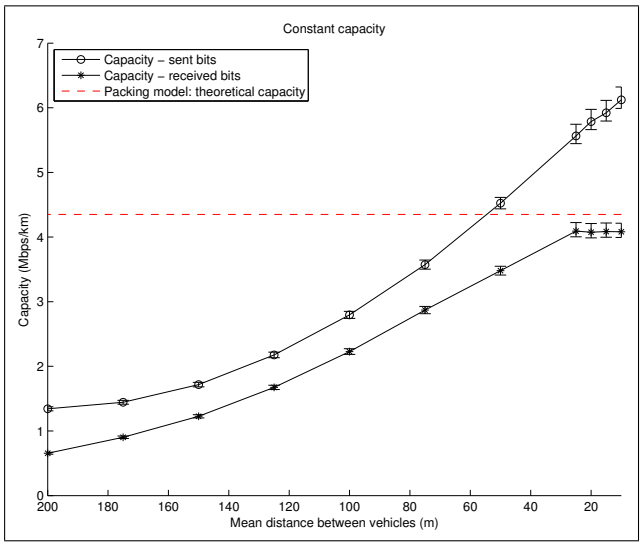

(a) Constant inter-distance.

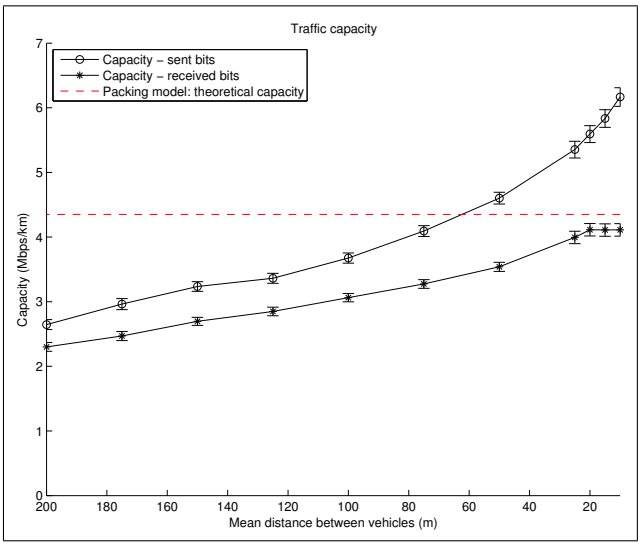

(b) Traffic simulator.

Fig. 12. Scenario from experimentations: capacity.

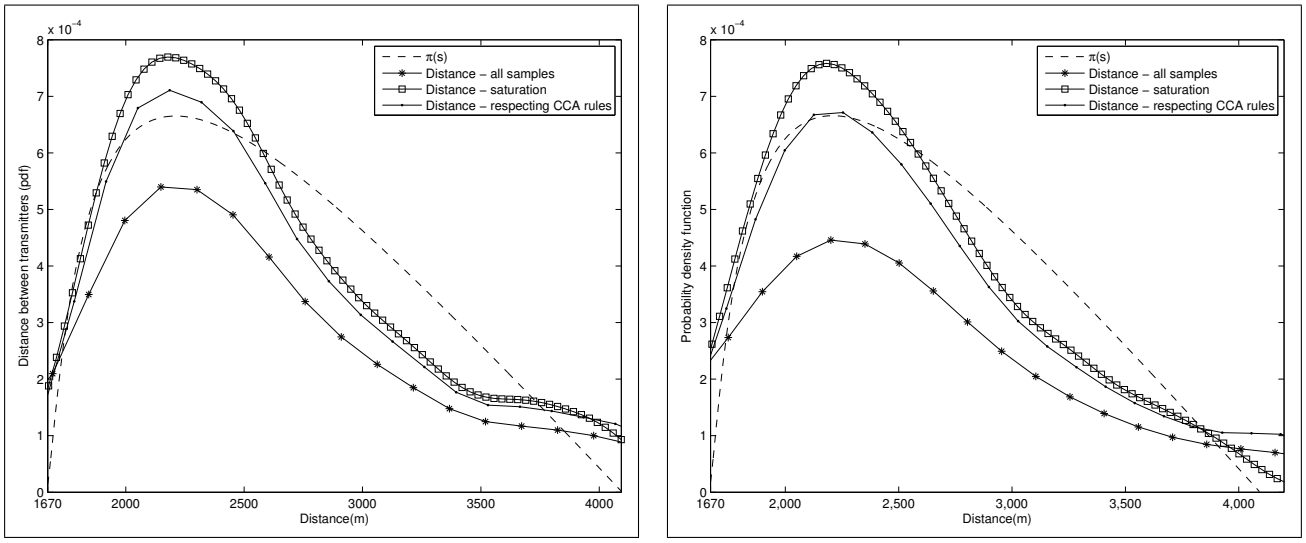

(a) Constant inter-distance. (b) Traffic simulator.

Fig. 13. No fading case: distribution of the distances between concurrent transmitters.

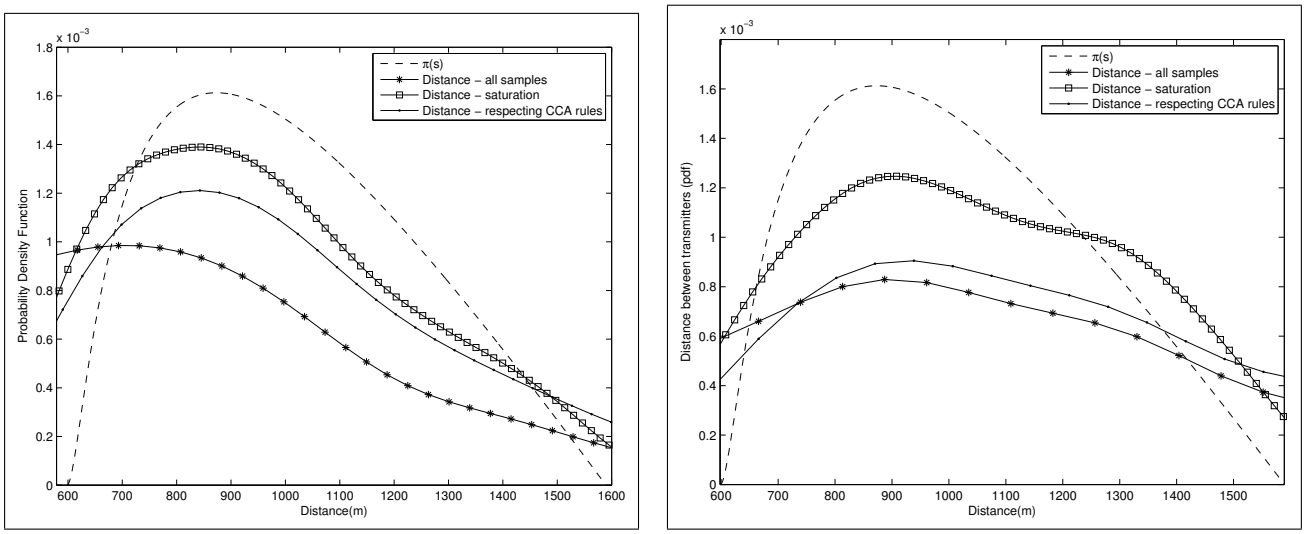

(a) Constant inter-distance. (b) Traffic simulator.

Fig. 14. Scenario from experimentations: distribution of the distances between concurrent transmitters.

of the highway for both scenarios. Each point in the different figures are computed as the mean of 100 simulations and are presented with a confidence interval at 95%.

We considered two kinds of traffic of vehicles. First, we assumed that the distance between the vehicles is constant. Then, we used our own traffic simulator to inject realistic vehicle locations into NS-3. Our micro-simulator emulates drivers' behavior on a highway (drivers are limited to accelerating, braking and changing lanes). A desired speed is associated with each vehicle. It corresponds to the speed that the driver would reach if he was alone in his lane. If the driver is alone (the downstream vehicle is sufficiently far), he adapts his acceleration to reach his desired speed (free flow regime). If he is not alone, he adapts his acceleration to the vehicles around (car following regime). He can also change lanes if the conditions of another lane seem better. All these decisions are functions of traffic condition (speed and distance) and random variables used to introduce a different behavior for each vehicle. This kind of simulation is called micro simulation [28], and the model we used is presented in detail in [29]. The model has been tuned and validated with regard to real data collected on a highway. For these simulations, we simulated a road/highway with 2 lanes. The desired speed of the vehicles follows a Normal distribution with mean 120 km/h and standard deviation $\sigma = 10$. The distance shown on the x-axis in the figures (traffic cases) corresponds to the mean distance between two successive vehicles. It varies from 800 to 10 meters.

B. Results on capacity

The theoretical capacity that is shown in the figures is computed from equation (7). The upper bound is 1.64 Mbps/km

for the first scenario, and 4.3 Mbps/km for the scenario from experimentations. In this equation, the mean time to transmit a frame T, is computed as the sum of AIFS (Arbitration Inter-Frame Space) equals to $71\mu s$, the backoff time equals to $n \times time\_slot$ (we choose $n = 1.5$ as this number is drawn in $[0, 3]$ for the highest priority) leading to $19.5\mu s$, the preamble duration and the time to transmit the frame header ($75\mu s$), and the time to transmit the payload ($533\mu s$). The final value of T is then $698\mu s$. This value is then used in Equation (7) to estimate the theoretical capacity.

1) No fading case: We plotted the capacity for this first scenario in Figure 11. The two figures correspond to the two kind of traffic: constant inter-distances and trajectories generated by the traffic simulator. We plotted two curves that correspond to the number of bits that has been sent (capacity - sent bits), and received by the neighbor of the sender (capacity - received bits). The theoretical bound, which equals approximately to 1.6 Mbps/km in this case, is very accurate and is reached even for very low density of traffic (for inter-distances less or equal to 100 meters).When the vehicles density increases, the number of sent bits becomes significantly greater than our bound. Indeed, the great number of vehicles willing to access the medium causes collisions, i.e. they select the same backoff and transmit at the same time. Consequently, a certain number of transmissions do not respect CCA rules leading to a greater number of transmitters and sent bits compared to our model. Nevertheless, it appears that most of these transmissions fail, leading to a number of received bits that are very close to the theoretical capacity. We can observe that for one point, the number of received bits exceeds the theoretical capacity. It is caused by transmissions that succeed even if they do not respect the CCA rule.

2) Scenario from experimentations: In Figure 12, we show the results on capacity for the scenario using the radio model from experimentations. The capacity estimated from simulations reaches approximately 4 Mbps/km whereas the theoretical bound is 4.3 Mbps/km. We plotted more points when the vehicles density is high. It allows us to observe that capacity stays constant (reaches its limit) when the mean inter-distance between vehicles is less than 25 meters. The bound is reached for smaller inter-distances (greater vehicles density) with regard to the previous scenario because the CCA distance (distance at which a transmission is detected) is smaller. The capacity is greater for the same reason.

Simulations show that our upper theoretical bound is pertinent as all simulations leads to similar but lower capacity. The theoretical capacity is achievable for traffic density greater than approximately 300 meters for the case without fading, and 30 meters for the other one. The difference is due to the radio range and CCA detection distance that is lower in the second scenario, leading to a better spatial reuse. Consequently, the maximum achievable capacity requires a denser distribution of vehicles. But, a density of 33 vehicles/km ($\frac{1}{0.03}$ veh/km) does not correspond in practice to a dense traffic scenario in a multi-lane highway or road. This bound is accurate, with less than 5% of errors for the scenario without fading, and less than 10% with the radio model from experimentations. Therefore, the packing model offers a good approximation of the maximum feasible capacity. This bound is thus almost reachable for the considered scenarios, but distances between transmitters and the considered receivers were favorable. For greater distances, congestion and fading may decrease the observed throughput with regard to this bound. The impacts of fading, congestion, and vehicular traffic are discussed in details below, where we compare the theoretical distance between transmitters with the empirical one.

C. Distribution of distances

In Figures 13 and 14, we plotted the distance distributions obtained with NS-3 and $\pi(s)$ given in Proposition 2. The abscissa is the interval $[S(D), D]$ (meters) given in Section V. We collected distances between transmitters from 100 simulations. For each simulation, we collected the distances between the transmitters and we plotted the corresponding empirical probability density function. We considered 3 cases: the case respecting CCA rules, saturation, and all samples. In the curve "respecting CCA rules", we neglected the distances which are lower than the theoretical minimum distance between two transmitters $S(D)$. Obviously, such a case corresponds to a collision, where two nodes competing for the medium access to the channel at the same time. For the saturation case, we did not take into account distances greater than D (we neglect region where the radio channel is idle). For the last case, we kept all the samples. The shapes of all distributions fit well with the Markovian model distribution $\pi(s)$, especially in case of saturation. Nevertheless, we cannot deny that we observe a difference. Indeed, it is very difficult to reach the absolute saturation condition where the medium is busy at every location, all the time. Sometimes, a vehicle satisfied CCA condition but it was on back-off stage, and does not transmit data. Therefore, there are regions where the medium is idle. Moreover, we observed that in case of realistic traffic, when the density becomes extremely dense (200 veh/km), local traffic jams appear. It leads to a very dense highway section (the jam), followed by a very sparse section. This strong inhomogeneity, generated by realistic traffic, explains the gap with our model. However, in the case of constant distances, the theoretical curves present only a small difference with simulations. It empirically proves that the Markovian model corresponds to a case where the CCA rule is respected by all nodes (no collisions), and where the medium is spatially busy. Even if these conditions are not feasible in practice, our Markovian model still offers accurate approximation for the distance distribution.

VIII. CONCLUSION

This study aims to propose realistic models that could be used as tools for dimensioning and parameterizing of VANET applications. The first model was used to estimate the VANET capacity, and the second deals with transmitter inter-distances, i.e. channel spatial reuse. We performed simulations as realistic as possible, combining the network simulator NS-3, a radio model obtained from real experimentations, and a traffic simulator. Comparisons between the theoretical capacity and the simulations have shown that our bound is achievable.

It empirically proves that these models capture the underlying mechanism limiting the capacity and setting the spatial reuse of the VANET. Our models are thus sufficiently accurate to offer a parameterizing tool for applications.

This work may be improved in different ways. The distribution of the distance between two transmitters can be used to evaluate Interference, Bit or Frame Error Rates. Packing models can be extended in order to take into account multi-path and fading properties of wireless links. Another improvement of our model should be to consider obstacles or more generally OLOS (Obstructed Line of Sight) between transmitters and nodes performing CCA. It may be done through the use of different path-loss functions, one will model LoS (Line of Sight) meaning that there is no intermediate obstacles/vehicles, and another one will model OLOS (Obstructed Line of Sight). Also, models could be improved to take into account sub-mechanisms of CSMA/CA (backoff, collisions, etc.). This latter proposition will require developing much more complex models than the ones presented in this paper.

REFERENCES

[1] Lee Armstrong and Wayne Fisher. Status of project ieee 802.11 task group p. wireless access in vehicular environments (wave). http://grouper.ieee.org/groups/802/11/Reports/tgp_update.htm.

[2] Hannes Hartenstein and Kenneth Kenneth Laberteaux. *VANET Vehicular Applications and Inter-Networking Technologies*. Wiley, 2009.

[3] S. Demmel, D. Gruyer, and A. Rakotonirainy. Comparing cooperative and non-cooperative crash risk-assessment. In *IEEE Intelligent Vehicles Symposium (IV'13)*, Gold Coast, Australiaa, 2013.

[4] A. Renyi. On a one-dimensional problem concerning random space-filling. *Publ. Math. Inst. Hung. Acad. Sci.*, 3:109–127, 1958.

[5] Network simulator 3 - ns3. http://www.nsnam.org.

[6] P. Gupta and P. Kumar. Capacity of wireless networks. *IEEE Transactions on Information Theory*, 46(2):388–404, 2000.

[7] M. Franceschetti, O. Dousse, D. Tse, and P. Thiran. Closing the gap in the capacity of wireless networks via percolation theory. *IEEE Transactions on Information Theory*, 53(3):1009–1018, 2007.

[8] O. Dousse and P. Thiran. Connectivity vs capacity in dense ad hoc networks. In *23rd IEEE Conference on Computer Communications (INFOCOM 2004)*, Hong Kong, China, March 2004.

[9] V. Mhatre, C. Rosenberg, and R. Mazumdar. On the capacity of ad-hoc networks under random packet losses. *IEEE Transactions on Information Theory*, 55(6):2494–2498, 2009.

[10] Lien-Wu Chen, Weikuo Chu, Yu-Chee Tseng, and Jan-Jan Wu. Route throughput analysis with spectral reuse for multi-rate mobile ad hoc networks. *J. Inf. Sci. Eng.*, 25(5):1593–1604, 2009.

[11] A. Busson and G. Chelius. Point processes for interference modeling in csma/ca ad-hoc networks. In *Sixth ACM International Symposium on Performance Evaluation of Wireless Ad Hoc, Sensor, and Ubiquitous Networks (PE-WASUN 2009)*, Tenerife, Spain, October 2009.

[12] Serkan Ozturk, Jelena Misic, and Vojislav B. Misic. Capacity limits in a variable duty cycle ieee 802.11p-based vanet. *Wireless Communications and Mobile Computing*, 12(18):1530–8677, 2012.

[13] M.G. Rubinstein, F. Ben Abdesslem, M.D. de Amorim, S.R. Cavalcanti, R. Dos Santos Alves, L.H.M.K. Costa, O.C.M.B. Duarte, and M.E.M. Campista. Measuring the capacity of in-car to in-car vehicular networks. *IEEE Communications Magazine*, 47(11):128–136, 2009.

[14] Chiara Buratti, Alberto Zanella, and Roberto Verdone. On the capacity of a csma-based multi-hop linear network with poisson distributed nodes. In *73rd IEEE Conference on Vehicular Technology (VTC Spring 2011)*, Budapest, Hungary, May 2011.

[15] Hossein Pishro-Nik, Aura Ganz, and Daiheng Ni. The capacity of vehicular ad hoc networks. In *45th Annual Allerton Conference on Communication, Control and Computing*, Allerton, USA, September 2007.

[16] Mohammad Nekaoui, Ali Eslami, and Hossein Pishro-Nik. Scaling laws for distance limited communications in vehicular ad hoc networks. In *IEEE International Conference on Communications (ICC 2008)*, Beijing, China, May 2008.

[17] Miao Wang, Hangguan Shan, Lin X. Cai, Ning Lu, Xuemin (Sherman) Shen, and Fan Bai. Throughput capacity of vanets by exploiting mobility diversity. In *IEEE International Conference on Communications (ICC 2012)*, pages 4980–4984, Ottawa, Canada, 2012.

[18] Lili Du, Satish Ukkusri, Wilfredo F. Yushimito Del Valle, and Shivkumar Kalyanaraman. Optimization models to characterize the broadcast capacity of vehicular ad hoc networks. *Transportation research. Part C, Emerging technologies, Elsevier*, 17(6):571–585, 2009.

[19] P. Jacquet and P. Muhlethaler. Mean number of transmissions with csma in a linear network. In *72nd IEEE Vehicular Technology Conference (VTC 2010-Fall)*, pages 1 –5, sept. 2010.

[20] P. Hall. *Introduction To the Theory of Coverage Processes*. Wiley, 1988.

[21] Lin Cheng, B.E. Henty, D.D. Stancil, Fan Bai, and P. Mudalige. Mobile vehicle-to-vehicle narrow-band channel measurement and characterization of the 5.9 ghz dedicated short range communication (dsrc) frequency band. *Selected Areas in Communications, IEEE Journal on*, 25(8):1501–1516, Oct. 2007.

[22] Vikas Taliwal, Daniel Jiang, Heiko Mangold, Chi Chen, and Raja Sengupta. Empirical determination of channel characteristics for dsrc vehicle-to-vehicle communication. In *Proceedings of the 1st ACM International Workshop on Vehicular Ad Hoc Networks*, VANET '04, pages 88–88, New York, NY, USA, 2004. ACM.

[23] The mad wi-fi project. http://madwifi-project.org/.

[24] D. Vonk Noordegraaf, K. M. Malone, and R. Van Katwijk. Accelerating cooperative systems development through the grand cooperative driving challenge. In *16th Intelligent Transport System World Congress (ITS 2009)*, Stokholm, Sweden, 2009.

[25] European telecommunications standards institute. http://www.etsi.org/.

[26] Federal communications commission. http://www.fcc.gov/.

[27] A. Ndjeng Ndjeng, A. Lambert, D. Gruyer, and S. Glaser. Experimental comparison of kalman filters for vehicle localization. In *IEEE Intelligent Vehicles Symposium (IV'09)*, pages 441–446, Xian, China, 2009.

[28] S. Druitt. An introduction to microsimulation. *Traffic engineering and control*, 39(9), 1998.

[29] Kazi I. Ahmed. *Modeling Drivers' Acceleration and Lane Changing Behavior*. PhD thesis, Massachusetts Institute of Technology, 1999.

[30] Persia Diaconis and David Freedman. On markov chains with continuous state space. *Mathematics statitics Library, University of California Berkeley*, (501):1–11, 1995.

APPENDIX A. PROOF OF PROPOSITION 1.

We show that $\lim \frac{m(L)}{L} \rightarrow constant$ when $L \rightarrow +\infty$. $m(L)$ is the mean number of points in the interval $[0, L]$, but it does not count the two points at 0 and L. First, we prove that $m(L)$ is a super-additive function, i.e. $m(L) \geq m(s) + m(L-s)$ for all $s \in (0, L)$. If $L < D$ then $m(L) = m(s) = m(L-s) = 0$ and the assertion is true. To prove the super-additivity for $L > D$, it suffices to note that, for $s \in [v(L), L - v(L)]$, $m(s)$ and $m(L-s)$ originally defined as the mean number of points in $[0, s]$ and $[0, L-s]$ are also equal to the mean number of points in the sets $[v(s), s - v(s)]$ and $[s + v(L-s), L - v(L-s)]$. Obviously, the mean number of points in $[v(L), L - v(L)]$ is greater than the sum of the points in two of its sub-intervals. Finally, if $s \in [0, v(L)]$ (respectively $\in [L - v(L), L]$), $m(s)$ (resp. $m(L-s)$) is nil and the remaining interval $[s + v(L-s), L - v(L-s)]$ (resp. $[v(s), s - v(s)]$) is a subset of $[v(L), L - v(L)]$.

$m(L)$ being super-additive and according to the Fekete Lemma, $\frac{m(L)}{L}$ converges to a finite or an infinite limit when $L \rightarrow +\infty$. To prove that the limit is finite, we need to show that $\exists A = constant \geq 0$ such that $m(L) \leq AL$. By definition, the minimal distance between two successive points is $\frac{D}{2}$. The mean number of points in $[0, L]$ is thus less than $\frac{L}{\frac{D}{2}}$. $\frac{m(L)}{L}$ is thus bound by a positive constant. Therefore, the limit is finite.

APPENDIX B. PROOF OF PROPOSITION 2.

First, we prove that if the initial distribution of the Markov chain (the distribution of ξ_1) is π, ξ_n follows the distribution π for all $n > 0$. It suffices to show that π is the stationary distribution for this chain. We need to prove that

$$\pi(s) = \int_{S(D)}^{D} f_{\xi_n|\xi_{n-1}=y}(s)\pi(y)dy \tag{14}$$

with $\pi(s) = a\left(D - S(s)\right)^2 (D - s)$ and $f_{\xi_n|\xi_{n-1}=y}(s)$ given by Equation (11).

We get,

$$\begin{aligned}
&\int_{S(D)}^{D} f_{\xi_n|\xi_{n-1}=y}(s)\pi(y)dy \\
&= \int_{S(D)}^{D} \left(\frac{-2}{(D-S(y))^2}s + \frac{2D}{(D-S(y))^2}\right) && (15)\\
&\times 1_{s\in[S(y),D]} a(D-y)(D-S(y))^2 dy && (16)\\
&= 2a(D-s)\int_{S^{-1}(s)}^{D}(D-y)dy && (17)\\
&= a\left(D-s\right)\left(D-S^{-1}(s)\right)^2 && (18)
\end{aligned}$$

where $S^{-1}(.)$ is the inverse function of $S(.)$. This function exists since due to the properties of the function $l(.)$, $S(u)$ is bijective, differentiable and strictly decreasing in $[S(D), D]$. To conclude, note that $S^{-1}(x) = S(x)$. It can be proved by considering the definition of $S(.)$ given by Equation (9). We get,

$$\begin{aligned}
&a\left(D-s\right)\left(D-S^{-1}(s)\right)^2 \\
&= a\left(D-s\right)\left(D-S(s)\right)^2 = \pi(s)
\end{aligned} \tag{19}$$

Also, we prove that ξ_n converges in total variation (it implies convergence in distribution) to π for any initial distribution of ξ_1 in $(S(D), D]$. We apply the Theorem 1 in [30] to prove this convergence. Since we have proved that π was the stationary distribution, it suffices to prove that the kernel P of this Markov chain is strongly $\pi-$irreducible, i.e. $\forall x \in (S(D), D]$ and $A \subset [S(D), D]$ with $\pi(A) > 0$, there is a positive integer n_{xA} such that $P^n(x, A) > 0\ \forall n \geq n_{xA}$. In our case, $\pi(A) > 0$ with $A \subset [S(D), D]$ is equivalent to $\nu(A) > 0$ where $\nu(.)$ is the Lebesgue measure in $\mathbb{R}^+$. The kernel P describes the transition probabilities, in our case it is formally defined as:

$$P(x, A) = \int_A f_{\xi_2|\xi_1=x}(y)dy \tag{20}$$

with $A \subset [S(D), D]$. $P^n(.,.)$ is the distribution of ξ_n $(n > 1)$ given ξ_1. It may be defined recursively:

$$P^n(x, A) = \int_{S(D)}^{D} P(x, dy)P^{n-1}(y, A) \tag{21}$$

First, note that if $P^m(x, A) > 0$ with $m > 0$, $P^n(x, A) > 0$ $\forall n \geq m$. It can be easily proved by recurrence: since $P^m(x, A) > 0\ \forall y \in [S(D), D]$ and $P(x, dy) = f_{\xi_2|\xi_1=x}(y)dy$ with $f_{\xi_2|\xi_1=x}(y) > 0\ \forall y \in [S(x), D]$, $P^{m+1}(x, A)$ expressed as

$$P^{m+1}(x, A) = \int_{S(D)}^{D} P(x, dy)P^m(y, A) \tag{22}$$

will be positive if $\nu([S(x), D]) > 0$, in other words if $x > S(D)$. We prove now that $P^2(x, A)$ for all $x \in [S(x), D]$ and $A \subset [S(x), D]$ with $\nu(A) > 0$. n_{xA} can thus be chosen equal to 2. Let $a = min\{u, u \in A\}$,

$$\begin{aligned}
P^2(x, A) &= \int_{S(D)}^{D} P(y, A)f_{\xi_2|\xi_1=x}(y)dy && (23)\\
&\geq \int_{S(min(x,a))}^{D} P(y, A)f_{\xi_2|\xi_1=x}(y)dy && (24)\\
&> 0
\end{aligned}$$

Indeed, $P(y, A) > 0$ and $f_{\xi_2|\xi_1=x}(y) > 0$ for all y in $[S(min(x, a)), D]$. Equation (24) is thus positive when $\nu([S(min(x, a)), D]) > 0$, i.e. when $x > S(D)$. This proves that the Markov chain is strongly $\pi-$irreducible, and thus μP^n converges in total variation to π when $n \to +\infty$ for any initial distribution μ in $(S(D), D]$.